Science Bulletin xxx (xxxx) xxx

Contents lists available at ScienceDirect

Science Bulletin

journal homepage: www.elsevier.com/locate/scib

Short Communication

NAT10-mediated mRNA N4-acetylcytidine modifications in mouse oocytes constitute a checkpoint of ovarian follicle development

Wen-Jing Wang [b,1], Yu-Ke Wu [b,1], Shao-Yuan Liu [b,1], Lu Chen [b,*], Hong-Bo Wu [c,*], Heng-Yu Fan [a,b,d,*]

[a] Zhejiang Key Laboratory of Precise Protection and Promotion of Fertility, Department of Obstetrics and Gynecology, Sir Run Run Shaw Hospital, School of Medicine, Zhejiang University, Hangzhou 310016, China
[b] Life Sciences Institute, Zhejiang University, Hangzhou 310058, China
[c] Department of Reproductive Medicine, Qinzhou Maternal and Child Health Care Hospital, Qinzhou 535099, China
[d] Center for Biomedical Research, Shaoxing Institute, Zhejiang University, Shaoxing 312000, China

ARTICLE INFO

Article history:
Received 27 May 2024
Received in revised form 4 July 2024
Accepted 13 September 2024
Available online xxxx

Proper ovarian follicle development, which is required for the maintenance of female fertility, is critical for the production of mature oocytes [1,2]. Meanwhile, the correct establishment of the epitranscriptome in oocytes is essential for precise gene repression and the acquisition of developmental competence [1–5]. The ac^4C modification is the third most abundant chemical modification in transcriptome [6,7]. NAT10, the only known writer of ac^4C, has been shown to participate in physiological and disease settings [6,8–11]. However, NAT10-targeted transcripts in oocytes as well as their functions in supporting folliculogenesis are poorly understood.

NAT10 was expressed in oocytes and granulosa cells (GCs) as early as the primordial follicle stage and was localized to the nuclei (Fig. 1a, arrows). Its expression level culminated in oocytes within the pre-antral and early antral follicles, indicating that NAT10 may play an important role in folliculogenesis. Immunofluorescence staining and western blotting revealed that NAT10 was highly expressed in growing oocytes and fully grown oocytes, and was expressed throughout the meiotic maturation process, with a decreasing trend as maturation progressed (Fig. 1b and Fig. S1a online). The *Nat10* expression level significantly increased during oocyte and follicle growth and was maintained at high levels during oocyte maturation (Fig. S1b online). To study the physiological functions of NAT10 and the ac^4C it mediates in follicle development, we crossed the *Nat10*-floxed mouse strain ($Nat10^{fl/fl}$) [12] with *Gdf9-Cre* and *Zp3-Cre* transgenic mice to specifically delete *Nat10* in oocytes, starting from the primordial and primary follicle stages, respectively (Fig. 1c). All animal experiments were conducted in accordance with the guidelines and regulations of the Zhejiang University, and the experimental protocol (ZJU20210252) was approved by the Zhejiang University Institutional Animal Care and Research Committee. Immunohistochemistry (IHC) results and western blotting confirmed that NAT10 was effectively deleted in oocytes starting from the primordial follicle stage in $Nat10^{fl/fl}$; *Gdf9-Cre* mice and from the primary follicle stage in $Nat10^{fl/fl}$; *Zp3-Cre* mice; however, the NAT10 expression pattern in GCs was intact in both strains (Fig. 1d and Fig. S1c online). For fertility tests, female mice in the control group gave birth to pups, whereas oocyte-specific *Nat10*-knockout female mice were completely infertile (Fig. 1e). The morphology of superovulated 4-week-old $Nat10^{fl/fl}$;*Gdf9-Cre* female mice was significantly abnormal (Fig. S1d–g online). In addition, hematoxylin and eosin (H&E) staining of paraffin-embedded ovarian samples indicated that *Nat10* knockout in oocytes ($Nat10^{fl/fl}$; *Gdf9-Cre* and $Nat10^{fl/fl}$; *Zp3-Cre*, $Nat10^{oo-/-}$) caused complete oocyte and follicle loss, resulting in premature ovarian failure (POF) at 3.5-months of age (Fig. 1f, g and Fig. S1h online). We collected ovary samples at different time points and found that $Nat10^{fl/fl}$; *Zp3-Cre* mice had smaller ovaries from the age of 10 weeks, and $Nat10^{fl/fl}$; *Gdf9-Cre* showed abnormalities at an earlier stage, from the age of 6 weeks (Fig. S1i, j online). We compared ovarian histology in 4-, 6-, 8-, and 10-week-old mice of different genotypes (Fig. 1h and Fig. S2 online). The ovaries of 4-week-old WT and $Nat10^{oo-/-}$ mice were morphologically similar, and the follicle counts showed no significant differences (Fig. S2a, b online). Ovarian histological analyses from the age of 6 weeks indicated that the number of primordial and antral follicles was significantly decreased in

* Corresponding authors.
E-mail addresses: l_chen@zju.edu.cn (L. Chen), 19587200@qq.com (H.-B. Wu), hyfan@zju.edu.cn (H.-Y. Fan).
[1] These authors contribute eqaully to this work.

https://doi.org/10.1016/j.scib.2024.09.020

Please cite this article as: W.-J. Wang, Y.-K. Wu, S.-Y. Liu et al., NAT10-mediated mRNA N4-acetylcytidine modifications in mouse oocytes constitute a checkpoint of ovarian follicle development, Science Bulletin, https://doi.org/10.1016/j.scib.2024.09.020

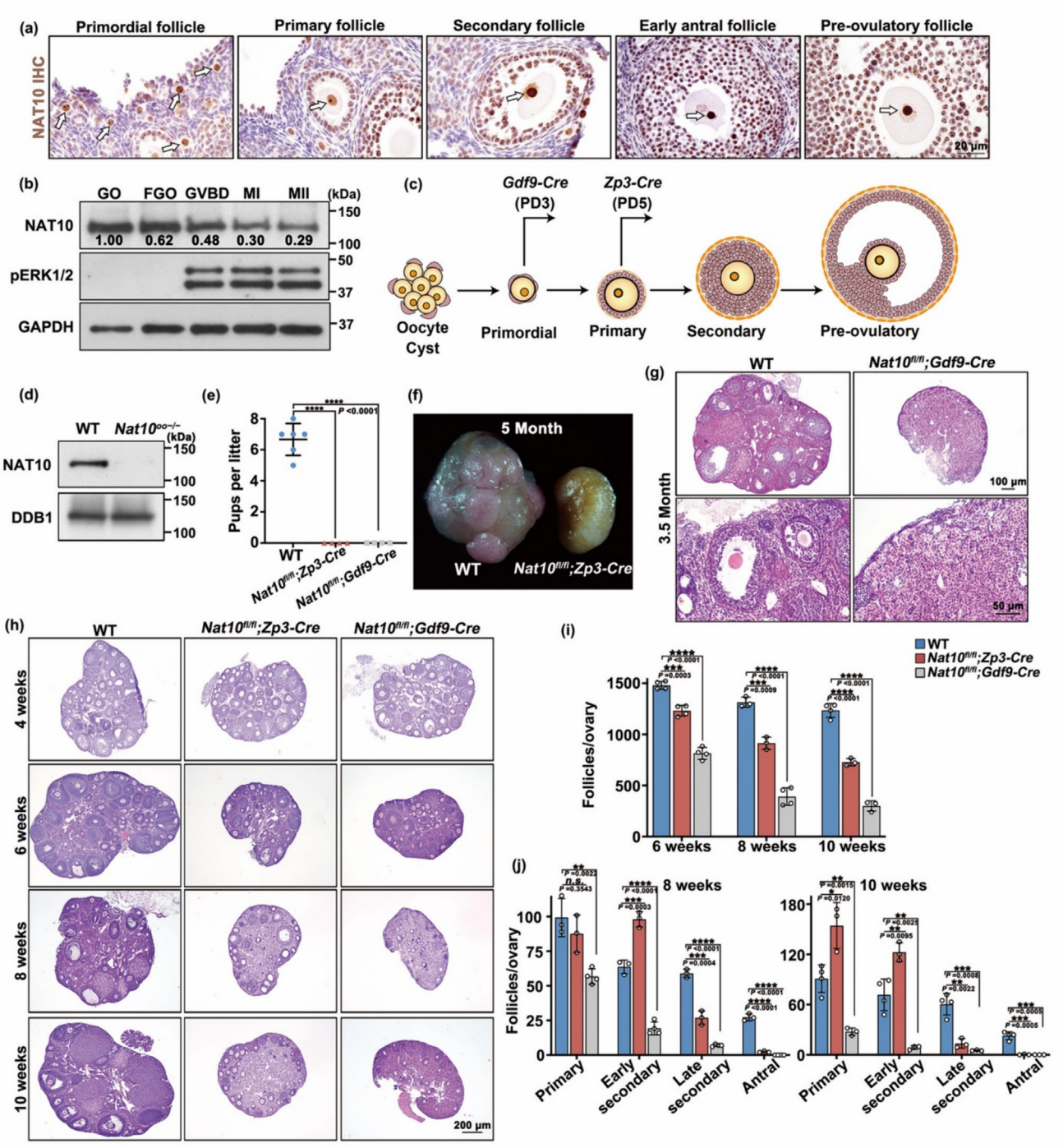

Fig. 1. *Nat10* deletion in oocytes causes follicle development defects and premature ovarian failure. (a) Immunohistochemistry (IHC) analysis of NAT10 in ovarian sections. Scale bars, 50 μm. The arrows indicate the nucleolus of oocytes in follicles. (b) Western blotting results showing NAT10 in mouse oocytes. (c) A schematic diagram showing ovarian follicular development and oocyte-specific *Nat10* knockout. (d) Western blotting results showing NAT10 levels in 100 fully grown oocytes isolated from control (WT) and *Nat10*$^{fl/fl}$;*Gdf9-Cre* (KO) mice. DDB1 was blotted as a loading control. (e) Fertility test of female mice. Error bars represent the standard error of the mean (SEM; $^{****}P < 0.0001$). (f) Representative ovarian images of 5-month-old control and *Nat10*$^{fl/fl}$;*Zp3-Cre* mice. (g, h) H&E staining results of ovarian sections at the indicated ages. (i) Serial primordial follicle counts in ovaries with the indicated ages and genotypes. (j) Serial follicle counts in ovaries with the indicated ages and genotypes. Data are shown as the mean ± SEM ($^{*}P < 0.05$, $^{**}P < 0.01$, $^{***}P < 0.001$, $^{****}P < 0.0001$, ns, not statistically significant.).

Nat10$^{oo-/-}$ mice (Fig. 1i and Fig. S2c, d online). Furthermore, *Nat10*$^{fl/fl}$; *Zp3-Cre* mice had fewer late-secondary follicles (with more than three layers of GCs) and a somewhat greater number of early-secondary follicles at 6 and 8 weeks of age (Fig. 1j and Fig. S2c–f online). These results indicate that NAT10 in oocytes is required for follicle development beyond the secondary follicle stage, except during the first wave of folliculogenesis.

We have detected a higher incidence of ac^{4}C modification in ovaries than in other tissues using dot blot and liquid chromatography-mass spectrometry [12]. We coupled acetylated RNA immunoprecipitation and next-generation-sequencing (acRIP-seq) to detect ac^{4}C modifications in the ovaries of adult WT mice (Fig. S3a online). After filtering for replication and removing IgG peaks, 8,210 candidate ac^{4}C peaks were detected in the three

independent biological replicates and they were predominantly enriched in the CDSs and 5′-UTRs of the transcripts, with a cytidine-containing motif significantly enriched in CA and CU repeats (Fig. 2a, b and Fig. S3b–c online). As shown in the genome browser of *Gdf9* (Fig. 2c), ac^{4}C signal peaks were enriched through acRIP. We further performed acRIP-qPCR assays to confirm the ac^{4}C peaks in the *Gdf9* gene, with a spike-in control (Fig. 2d and Fig. S3g online). ac^{4}C peaks were also identified in the following genes using acRIP-seq analysis and acRIP-qPCR assays (Fig. 2d and Fig. S3f, g online). We further optimized the linear amplification of complementary DNA ends and sequencing (LACE-seq) method for unbiased mapping of ac^{4}C sites at a high resolution in 50 fully grown oocytes, which we have shown to have high sensitivity and reliability. We compared the ac^{4}C transcripts found in ac^{4}C LACE-seq and acRIP-seq, and found that 1656 genes overlapped (Fig. 2e). Furthermore, we performed joint analyses of our ac^{4}C LACE-seq data with the acRIP-seq results to verify the reliability and reproducibility of the sequencing results (Fig. S3h–j online). Although the ac^{4}C signals detected by ac^{4}C LACE-seq decreased compared with acRIP-seq, the precision was still similar and reads on chromosome 7 showed similar specific peaks for ac^{4}C (Fig. S3j online). These results demonstrated that mRNAs of genes in oocyte involved in folliculogenesis have high levels of ac^{4}C.

To investigate the influence of *Nat10*-knockout on maternal mRNA abundance, we collected fully grown oocytes from 6-week-old WT and *Nat10*-knockout mice for transcriptome sequencing. The samples showed high correlations (Fig. S4a online) and the overall transcript levels of *Nat10*-knockout oocytes were lower than those of WT oocytes (Fig. S4b online) after calibrating data between different samples. A total of 245 genes were upregulated and 1541 were downregulated in *Nat10*-null oocytes compared to those in WT oocytes (Fig. S4c online), which was different with our 3-week-old oocytes' results. Thus, we analyzed the differentially expressed genes in 3-week-old to 6-week-old *Nat10*-null oocytes (Fig. 2f). Consistent with the proposed role of NAT10 in regulating RNA stability, more transcripts were downregulated than upregulated after *Nat10* knockout in oocytes. Moreover, the transcripts were downregulated to a greater extent in 6-week-old oocytes than in 3-week-old oocytes, suggesting a cumulative effect of age (Fig. 2f). In particular, most of the ac^{4}C-positive (ac^{4}C$^+$) transcripts were downregulated rather than upregulated after *Nat10* deletion, and the trend of downregulation intensified from the age of 3 to 6 weeks (Fig. 2g). The downregulated ac^{4}C$^+$ transcripts were enriched in biological process such as mRNA processing, regulation of translation, and RNA stability (Fig. S4d online). Deleting *Nat10* downregulated the expression of numerous oocyte-specific transcripts, including those encoding oocyte-derived paracrine factors, gap junction proteins, zona pellucida components, and Notch signaling ligands, as confirmed by RT-qPCR (Fig. S4e online). We also utilized the Integrative-Genomics-View software to search for target genes based on our LACE-seq datasets, and found that the ac^{4}C peaks in these genes were significantly decreased in *Nat10*-knockout oocytes (Fig. S5a online). Next, we performed mRNA stability assay by culturing WT and *Nat10*-null growing oocytes with 50 μmol L^{-1} α-amanitin to repress *de novo* gene transcription. All the studied RNA transcripts showed accelerated degradation in *Nat10*-deleted oocytes (Fig. S5b online), indicating that NAT10 regulates the RNA stability of these oocyte genes through ac^{4}C-dependent manner.

Oocyte-specific paracrine factors play key roles in promoting follicle growth (Fig. S6a online) [13]. *Nat10*-deletion altered the expression pattern of many oocyte-derived factors (Fig. S5), which are involved in the oocyte-GC dialog and important for folliculogenesis (Fig. 2i–k). In *Nat10*-depleted oocytes, we detected decreased protein levels in GDF9, BMP15 and CX37 (Fig. 2i–k), which are essential for somatic cell-ocyte communications. Maternal MSY2, PABPN1 and ZAR1 play essential roles in oocyte growth and maturation, their expression level decreased in oocytes after *Nat10* knockout (Fig. 2j, k). Collectively, *Nat10*-deletion in oocytes resulted in the downregulation of folliculogenesis-related genes containing ac^{4}C peaks at the protein level, in addition to the mRNA level.

NAT10 is responsible for the ac^{4}C modification of target transcripts; however, there is no direct evidence to clarify that NAT10 regulates the translational efficiency of these studied genes in ac^{4}C-modification-dependent manner. We utilized PACES software to predict the probable ac^{4}C sites of these target genes [14], and found ac^{4}C modification sites in the 5′ UTR, CDS, and/or 3′ UTR regions of *Gja4*, *Msy2*, *Pabpn1*, *Zar1*, and *Jag1* mRNAs, especially in the CDS region (Table S8 online). We introduced multiple C-to-A/U/G mutations into the conserved ac^{4}C peaks, without altering the encoded amino acid residues (Fig. 2l and Fig. S6d online). These plasmids were constructed and transfected into 293 T cells. Western blotting results indicated that the ac^{4}C site mutations in *Gja4*, *Pabpn*1, and *Jag1* CDSs decreased their expression levels (Fig. 2m and Fig. S6c–g online). To further investigate the biological relevance of ac^{4}C modifications to translation in mammalian oocytes, we cloned mouse *Gdf9* and *Gja4* CDSs and ligated them into the pRK5-*Flag-Gfp* vector. The mRNA was then *in vitro*-transcribed with the presence of CTPs (as negative control) or acetylated CTPs (ac^{4}CTPs) and microinjected into GV stage-arrested oocytes. The microinjected oocytes were cultured for 12 h within milrinone (Fig. S6h online). The translational efficiency of FLAG-GFP in oocytes was determined using epifluorescence and western blotting. The results showed that ac^{4}C-positive transcripts had higher protein expression levels than ac^{4}C-negative transcripts at the GV stage (Fig. 2n-q and Fig. S6i, j online), indicating that ac^{4}C modifications in the CDSs of folliculogenesis-related target genes positively affect their translational activity.

We further explored the mechanism by which *Nat10*-deletion in oocytes causes follicular developmental defects. The number of dividing GCs labeled with pHH3 and Ki67 was less in the secondary follicles of *Nat10*$^{po-/-}$ mice compared with those of control mice (Fig. S7-8 online). On the contrary, no increase in GC apoptosis or

Fig. 2. NAT10-mediated ac^{4}C modification regulates folliculogenesis. (a) Number of ac^{4}C peaks parsed by location within coding sequences (CDSs) or untranslated region (UTRs) for all acetylated transcripts. (b) Pie charts indicating the percentage of peaks within promoters or UTRs in the acetylated transcripts. (c) Browser view of ac^{4}C peaks in the *Gdf9* mapped to the mouse reference genome to the mRNA sequences. (d) acRIP-PCR results for indicated transcripts showing ac^{4}C peaks in comparison with globin and *Gapdh* as controls. (e) Venn diagram showing the overlap of acRIP-seq and ac^{4}C LACE-seq identified genes with ac^{4}C peaks. (f) Significantly differentially expressed genes between WT and *Nat10*-null oocytes from 3 and 6 weeks old mice. (g) A total of 2366 ac^{4}C$^+$ transcripts were jointly analyzed using RNA-seq data showing the level changes of these transcripts in *Nat10*-null oocytes from 3 to 6 weeks of age. (h) RT-qPCR results showing the transcript level changes in WT and *Nat10*-null oocytes. (i, j) Western blotting results showing the expression of folliculogenesis-related proteins in oocytes. Total proteins from 200 oocytes were loaded in each lane. (k) IHC results showing the expression of PABPN1, ZAR1 and CX37 in the ovaries. (l) Potential sites for ac^{4}C modification in mouse *Gja4* mRNA predicted by PACES software. (m) The WT and the ac^{4}C sites of mutant *Gja4* were transfected into 293 T cells and the HA-GJA4 level was determined by western blotting. (n) The expression of FLAG-GFP-fused *Cx37* CDSs in WT oocytes at 12 h after microinjection. (o, p) Relative GFP intensity and western blotting analysis showing the expression levels of FLAG-GFP-CX37 in microinjected oocytes. (q) Western blotting analysis showing the expression levels of FLAG-GFP-GDF9 in microinjected oocytes. (r, s) Western blotting showing the expression level of the indicated genes in secondary follicles isolated from ovaries at 8 weeks of age. (t) Quantitative RT-PCR results of mRNAs in GCs of secondary follicles isolated from ovaries at 8 weeks of age. *Actin* and actin were used as internal controls. (u) IHC staining of FOXO1 and 3β-HSD in ovaries of 8-week-old mice. Data are presented as the means ± SEM from at least three independent experiments and were compared using one-way analysis of variance (ANOVA). $^*P < 0.05$, $^{**}P < 0.01$, $^{***}P < 0.001$, $^{****}P < 0.0001$.

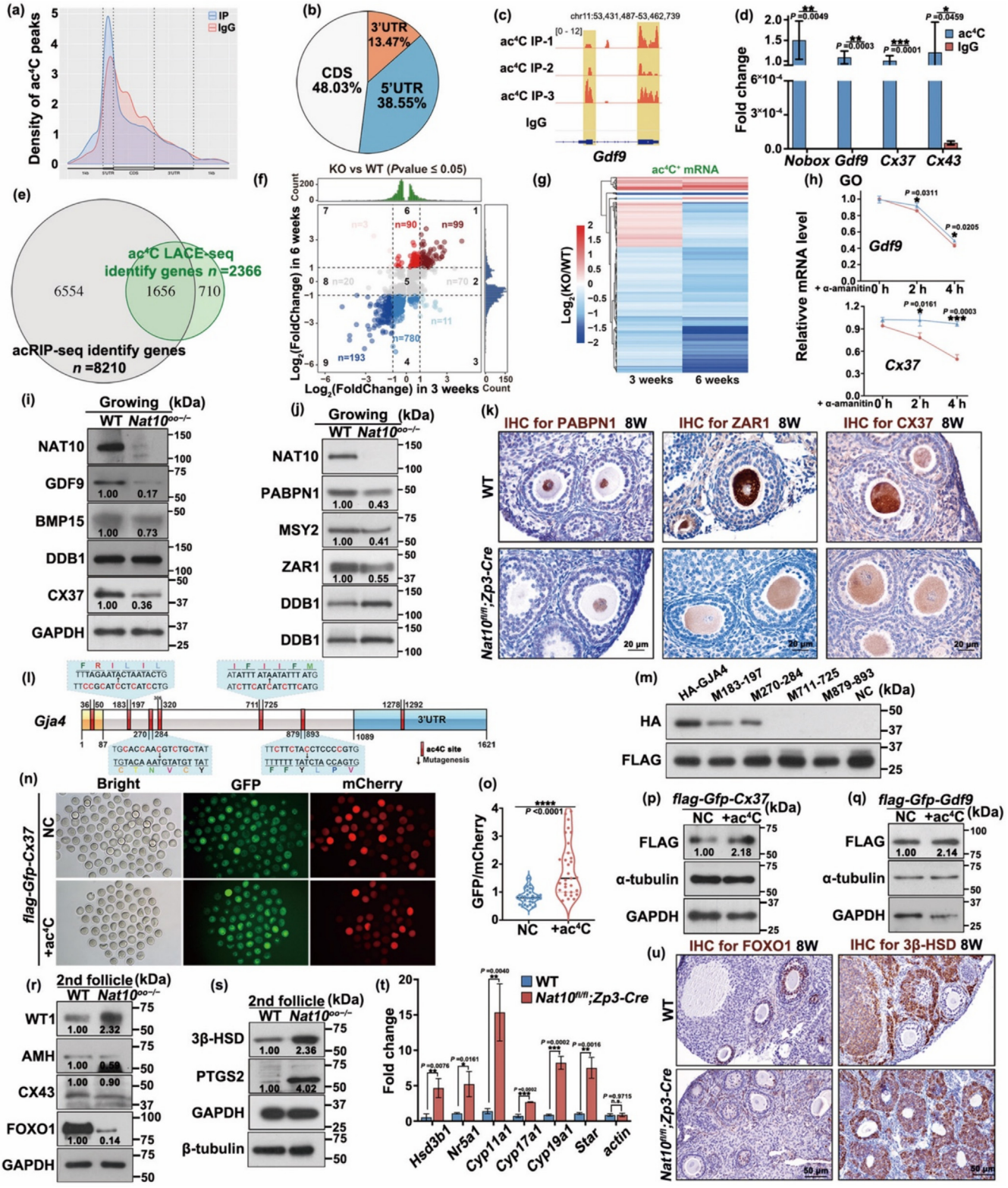
(a)
Density of ac4C peaks
IP
IgG
(b)
3'UTR 13.47%
CDS 48.03%
5'UTR 38.55%
(c)
chr11:53,431,487-53,462,739
ac4C IP-1
ac4C IP-2
ac4C IP-3
IgG
Gdf9
(d)
Fold change
ac4C
IgG
Nobox Gdf9 Cx37 Cx43
(e)
ac4C LACE-seq identify genes n =2366
6554
1656
710
acRIP-seq identify genes n =8210
(f)
KO vs WT (Pvalue ≤ 0.05)
Log2(FoldChange) in 6 weeks
Log2(FoldChange) in 3 weeks
n=90
n=99
n=20
n=70
n=11
n=780
n=193
(g)
ac4C+ mRNA
Log2(KO/WT)
3 weeks
6 weeks
(h)
GO
Relativve mRNA level
Gdf9
Cx37
+ α-amanitin
0 h
2 h
4 h
(i)
Growing (kDa)
WT Nat10oo-/-
NAT10
GDF9
BMP15
DDB1
CX37
GAPDH
(j)
Growing (kDa)
WT Nat10oo-/-
NAT10
PABPN1
MSY2
ZAR1
DDB1
(k)
IHC for PABPN1 8W
IHC for ZAR1 8W
IHC for CX37 8W
WT
Nat10fl/fl;Zp3-Cre
20 μm
(l)
Gja4
3'UTR
ac4C site
Mutagenesis
(m)
HA-GJA4
M183-197
M270-284
M711-725
M879-893
NC
HA
FLAG
(n)
Bright
GFP
mCherry
flag-Gfp-Cx37
NC
+ac4C
(o)
GFP/mCherry
NC
+ac4C
(p)
flag-Gfp-Cx37
NC +ac4C (kDa)
FLAG
α-tubulin
GAPDH
(q)
flag-Gfp-Gdf9
NC +ac4C (kDa)
FLAG
α-tubulin
GAPDH
(r)
2nd follicle (kDa)
WT Nat10oo-/-
WT1
AMH
CX43
FOXO1
GAPDH
(s)
2nd follicle (kDa)
WT Nat10oo-/-
3β-HSD
PTGS2
GAPDH
β-tubulin
(t)
WT
Nat10fl/fl;Zp3-Cre
Fold change
Hsd3b1
Nr5a1
Cyp11a1
Cyp17a1
Cyp19a1
Star
actin
(u)
IHC for FOXO1 8W
IHC for 3β-HSD 8W
WT
Nat10fl/fl;Zp3-Cre
50 μm

follicle atresia were detected (Fig. S9 online). Furthermore, we assessed whether GCs in *Nat10*$^{oo-/-}$ ovaries were functionally normal. The protein expression level of FOXO1 (a marker of GCs in growing follicles), anti-Müllerian hormone (AMH, a marker for GCs) and connexin 43 (CX43) were decreased in the GCs of secondary follicles in *Nat10*$^{oo-/-}$ mice (Fig. 2r), and even the mRNA levels of these genes were markedly lower (Fig. S10d online). Wilms tumor 1 (*Wt1*) is associated with GC-to-steroidogenic cell transformation, but both the protein and mRNA levels of WT1 increased in the secondary follicle GCs of 8-week-old *Nat10*$^{fl/fl}$; *Zp3-Cre* mice (Fig. 2r and Fig. S10d online). Steroidogenesis-related gene prostaglandin-endoperoxide synthase 2 (*Ptgs2*) and 3β-hydroxysteroid dehydrogenase (3β-HSD) was also detected in the GCs and theca-interstitial cells of *Nat10*$^{oo-/-}$ mice, and had a higher protein level in secondary follicles than those of WT mice (Fig. 2s–u and Fig. S10b, c online). The expression of GC-specific genes, including *Amh*, *Foxo1*, and *Foxl2* were decreased, whereas the steroidogenic genes *Hsd3b1*, *Nr5a1*, *Cyp11a1*, and *Star* were increased in the secondary follicle GCs of *Nat10*$^{oo-/-}$ mice (Fig. 2t and Fig. S10d online). These data indicate that the distinct gene expression patterns in GCs within arrested secondary follicles were disrupted, and the identity of GCs was changed by *Nat10* deletion in oocytes.

In summary, we report that *Nat10* deletion in mouse oocytes leads to specific arrest of follicular development at the secondary follicle stage, premature ovarian insufficiency, and female infertility. The reduction in the ac^{4}C modification in specific regions of mRNAs resulting from NAT10 knockout in oocytes impaired the stability and translational efficiency of the oocyte-derived factors' mRNAs, which led to the impairment of oocyte growth and even the regulation from oocytes to GCs. Our study revealed the unique and novel functions of ac^{4}C modifications in folliculogenesis and highlighted the cell non-autonomous function of *Nat10* in oocytes in controlling the developmental states of surrounding granulosa cells. This study demonstrates that NAT10-mediated ac^{4}C modification in oocytes constitutes a checkpoint for ovarian folliculogenesis beyond the secondary follicle stage.

Conflict of interest

The authors declare that they have no conflict of interest.

Acknowledgments

This work was supported by the National Key Research and Development Program of China (2021YFC2700100), the Natural Science Foundation of Zhejiang Province (LD22C060001), the National Natural Science Foundation of China (31930031), the fellowship of China National Postdoctoral Program for Innovative Talents (BX20230031), Beijing Natural Science Foundation (7244435).

Author contributions

Heng-Yu Fan and Hong-Bo Wu conceived, designed, and supervised the study. Wen-Jing Wang, Yu-Ke Wu, Shao-Yuan Liu and Lu Chen performed the research. Yuke Wu and Shao-Yuan Liu analyzed sequencing data. Wen-Jing Wang and Heng-Yu Fan wrote the manuscript.

Appendix A. Supplementary material

Supplementary data to this article can be found online at https://doi.org/10.1016/j.scib.2024.09.020.

References

[1] McGee EA, Hsueh AJ. Initial and cyclic recruitment of ovarian follicles. Endocr Rev 2000;21:200–14.
[2] Mu H, Zhang T, Yang Y, et al. METTL3-mediated mRNA N^6-methyladenosine is required for oocyte and follicle development in mice. Cell Death Dis 2021;12:989.
[3] Wu Y, Xu X, Qi M, et al. N^6-methyladenosine regulates maternal RNA maintenance in oocytes and timely RNA decay during mouse maternal-to-zygotic transition. Nat Cell Biol 2022;24:917–27.
[4] Frye M, Harada BT, Behm M, et al. RNA modifications modulate gene expression during development. Science 2018;361:1346–9.
[5] Roundtree IA, Evans ME, Pan T, et al. Dynamic RNA modifications in gene expression regulation. Cell 2017;169:1187–200.
[6] Arango D, Sturgill D, Alhusaini N, et al. Acetylation of cytidine in mRNA promotes translation efficiency. Cell 2018;175:e1824.
[7] Sas-Chen A, Thomas JM, Matzov D, et al. Dynamic RNA acetylation revealed by quantitative cross-evolutionary mapping. Nature 2020;583:638–43.
[8] Xie L, Zhong X, Cao W, et al. Mechanisms of NAT10 as ac4C writer in diseases. Mol Ther Nucleic Acids 2023;32:359–68.
[9] Jin G, Xu M, Zou M, et al. The processing, gene regulation, biological functions, and clinical relevance of N4-acetylcytidine on RNA: A systematic review. Mol Ther Nucleic Acids 2020;20:13–24.
[10] Jiang X, Cheng Y, Zhu Y, et al. Maternal NAT10 orchestrates oocyte meiotic cell-cycle progression and maturation in mice. Nat Commun 2023;14.
[11] Xiang Y, Zhou C, Zeng Y, et al. NAT10-mediated N4-acetylcytidine of RNA contributes to post-transcriptional regulation of mouse oocyte maturation *in vitro*. Front Cell Dev Biol 2021;9.
[12] Chen L, Wang WJ, Liu Q, et al. NAT10-mediated N4-acetylcytidine modification is required for meiosis entry and progression in male germ cells. Nucleic Acids Res 2022;50:10896–913.
[13] Gershon E, Dekel N. Newly identified regulators of ovarian folliculogenesis and ovulation. Int J Mol Sci 2020;21.
[14] Zhao W, Zhou Y, Cui Q, et al. Paces: Prediction of N4-acetylcytidine (ac^{4}C) modification sites in mRNA. Sci Rep 2019;9:11112.

Wen-Jing Wang received her B.S. degree in Biological Science from Northwest A&F University. She is a Ph.D candidate in Cell Biology at Zhejiang University, studying the mechanisms of mammalian germ cell development, particularly the posttranscriptional regulations of maternal RNAs.

Hong-Bo Wu received his M.D. and Ph.D. degrees in Reproductive Medicine from Guangxi Medical University. He is a director and professor at Qinzhou Maternal and Child Health Care Hospital. His research focuses on women's reproductive medicine and assisted reproduction.

Heng-Yu Fan received his Ph.D. degree in Reproductive Biology from Institute of Zoology, Chinese Academy of Sciences. He is a professor at Life Sciences Institute, Zhejiang University. His research focuses on mammalian female reproduction and the mechanism of zygotic developmental activation.